Alignment-free Sequence Comparisons via Approximate String Matching

Jian Chen[1*], Le Yang[2*], Lu Li[3], Steve Goodison[5], Yijun Sun[1, 2, 4†]

[1]Department of Computer Science and Engineering
[2]Department of Microbiology and Immunology
[3]Department of Oral Biology
[4]Department of Biostatistics
University at Buffalo, The State University of New York
Buffalo, NY 14203
[5]Department of Quantitative Health Sciences
Mayo Clinic, Jacksonville, FL 32224

Abstract

Motivation: Sequence comparison is a fundamental problem in bioinformatics and plays a key role in a wide range of applications. Alignment-free methods provide a computationally efficient alternative to alignment-based methods for large-scale sequence analysis. Several neural network-based methods have recently been developed for this purpose. However, due to the fact that the neural networks employed are not designed specifically for biological sequence analysis, existing methods do not perform well on sequences of varying lengths and are sensitive to the presence of insertions and deletions.

Results: In this paper, we describe the development of a new method, referred to as AsMac, that addresses the aforementioned issues. We proposed a novel neural network structure for approximate string matching for the extraction of pertinent information from biological sequences and an efficient gradient computation algorithm for training the constructed neural network. We performed a large-scale benchmark study using real-world data that demonstrated the effectiveness and potential utility of the proposed method.

Availability: Open-source software for the proposed method is developed and freely available at `www.acsu.buffalo.edu/~yijunsun/lab/AsMac.html`.

Supplementary information: Supplementary data are available at *Bioinformatics* online.

Bioinformatics
submitted on May 8, 2022

[*]Equal contribution
[†]Please address all correspondence to Dr. Yijun Sun (`yijunsun@buffalo.edu`).

1 Introduction

Quantifying pairwise sequence similarities is a key step in various bioinformatics analyses, including those for database search [1, 2], sequence annotation [3], and metagenomics [4--6]. Classic approaches to sequence analysis are based on sequence alignment, either global or local, pairwise or multiple sequence alignment. In this paper, we focus on global pairwise sequence alignment, for which the Needleman-Wunsch (NW) algorithm [7] is the optimal method. However, due to high computational complexity, the application of the NW algorithm is limited to small sequence datasets. With the advent of next-generation sequencing technology, the data generation capacity has increased dramatically, and the rapid accumulation of sequence data poses a serious challenge for data analysis and demands new computational algorithms for efficient data processing.

Over the past two decades, dozens of alignment-free approaches have been developed to provide computationally efficient alternatives to alignment-based approaches [8--11]. Commonly used methods can be broadly classified into two categories: 1) methods based on word frequency (e.g., k-mer [12], FFP [13], and CV [14]), and 2) methods based on substrings (e.g., ACS [15], Kr [16], and kmacs [17]). There also exist some methods based on information theory (e.g., IC-PIC [18]), but they are less commonly used. By transforming sequences into numerical vectors, alignment-free methods can be viewed as defining an implicit mapping function that projects sequences into an embedding space where pairwise sequence similarities are calculated. The methods in the first category are based on the statistics of fixed-length word frequency or on the information content of word frequency distributions, while the methods in the second category employ the similarities or differences of substrings in a pair of sequences. For substring-based methods, it is not necessary to specify a word length, and thus in general they can achieve better performance than those relying on a fixed word length. However, substring-based methods introduce new parameters (e.g., the number of mismatches in kmacs [17]) that cannot be easily estimated. Moreover, computing features of variable word lengths usually requires more complex data structures and thus is computationally more expensive [17]. A major limitation of the above methods is that they are all data-independent approaches, where distance measures are predefined based on various heuristics and thus can only provide rough approximations to alignment distances.

Recently, several attempts have been made to use neural networks to develop data-dependent approaches for alignment-free sequence comparison (e.g., SENSE [19] and NeuroSEED [20]). The basic idea is to use a neural network to learn an explicit mapping function through training and to map sequences onto an embedding space so that the mean square error between alignment distances and pairwise distances defined in the embedding space is minimized. Since the mapping function is learned through training, it has been demonstrated that data-dependent methods can offer much more accurate solutions than data-independent counterparts [19, 20]. Moreover, neural network-based approaches are computationally very efficient, and run even faster than the k-mer method [19]. The development of data-dependent approaches makes it

possible to develop and publish trained neural-network models for a specific task (e.g., metagenomics data analysis) that other researchers can use to process their own datasets. However, existing methods suffer from several major limitations. First, biological sequences under comparison usually have varying lengths, however, SENSE can only be applied to sequences of equal length, and NeuroSEED uses zero padding to make sequences have the same length, which is not biologically meaningful and can lead to poor performance. Second, early attempts used the convolutional neural network (CNN) for sequence comparison. CNN was designed mainly for image analysis [21] and cannot effectively model insertions and deletions—collectively called indels—due to the use of dot product to measure the similarity between a filter and a sequence. Although gated recurrent units and attention transformers have achieved great success for natural language data analysis [22, 23], it was found that they were inferior to CNN for biological sequence comparisons [20].

In this paper, we describe the development of a novel neural network-based method, referred to as AsMac, that addresses the aforementioned issues. Specifically, we used approximate string matching (ASM) to transform sequences into numeric vectors. Since ASM uses the edit distance to measure the similarity between a pattern and a sub-sequence, it is well suited for extracting pertinent information from biological sequences. To learn patterns from data *automatically*, we proposed a novel neural network structure for the implementation of approximate string matching and an efficient gradient computation algorithm for training the constructed neural network. We performed a large-scale experiment on real-world data that demonstrated the effectiveness and utility of the proposed method.

2 Methods

2.1 Overview

We propose a novel method that uses a Siamese neural network and approximate string matching for alignment-free sequence comparison. Fig. 1 depicts the overview of the proposed method. The basic idea is to use a neural network to project sequences into embedding vectors so that the difference between alignment distances and pairwise dissimilarities calculated in the embedding space is minimized. Since inputs and outputs are from the sequence and numerical domains, respectively, and are not directly comparable, we use a twin neural network—also called Siamese neural network [25]—to learn a mapping function. Specifically, given a pair of sequences $(\mathcal{S}_1, \mathcal{S}_2)$, each network takes one sequence as input and outputs $f(\mathcal{S}_1|\Theta)$ and $f(\mathcal{S}_2|\Theta)$ as the embedding vectors of the two sequences, respectively. Here, f is the mapping function, and Θ is the parameters of the network to be optimized. To form the twin network, we propose a novel neural network for approximate string matching (detailed below). To train the network, we compute the alignment distance $d_a(\mathcal{S}_1, \mathcal{S}_2)$ by using the Needleman-Wunsch (NW) algorithm and the cosine distance of the embedding vectors as the embedding distance $d_e(f(\mathcal{S}_1|\Theta), f(\mathcal{S}_2|\Theta))$, and optimize the neural network by using backpropagation to minimize the mean square error

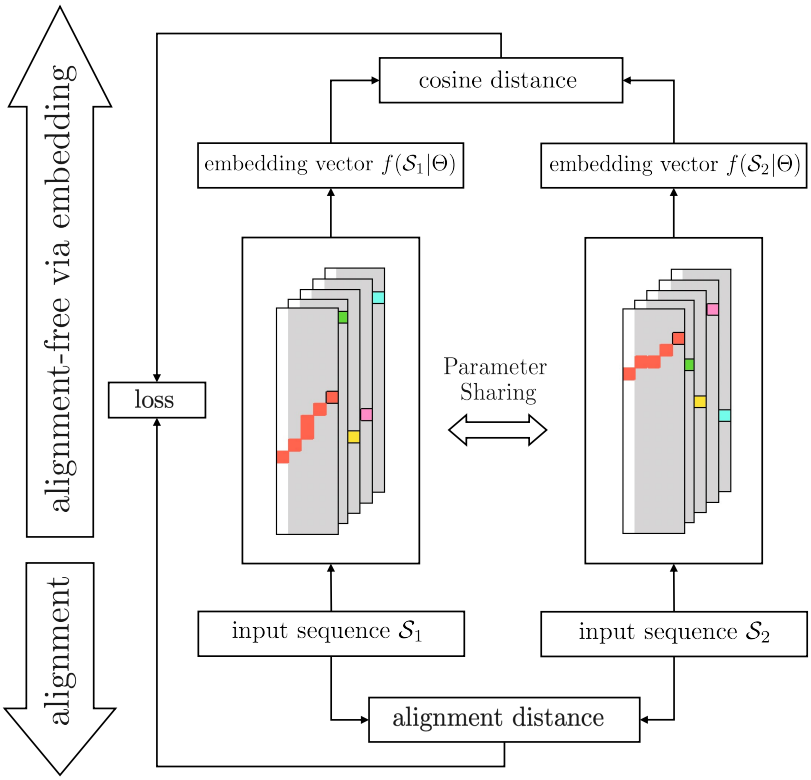

Figure 1: Overview of the proposed method that combines a Siamese neural network and approximate string matching for alignment-free sequence comparison and its training process.

given by

$$C(\mathbf{\Theta}) = \sum_{i,j} \left(d_e(f(\mathcal{S}_i|\mathbf{\Theta}), f(\mathcal{S}_j|\mathbf{\Theta})) - d_a(\mathcal{S}_i, \mathcal{S}_j)\right)^2 \ . \tag{1}$$

In the training process, the twin networks are forced to share the same parameters, including both initialization and gradient descent updates. Once Siamese neural network is optimized, one of the networks is used to project sequences into embedding vectors.

2.2 Approximate String Matching

We start by giving a brief description of the approximate string matching (ASM) algorithm. Let $\mathcal{S} = s_1 \dots s_L$ be a sequence and $\mathcal{P} = p_1 \dots p_M$ be a pattern. We aim to identify a sub-sequence in $\mathcal{S}$ that has the minimum edit distance to pattern $\mathcal{P}$ among all subsequences of $\mathcal{S}$. Dynamic programming provides the optimal solution for this purpose [24]. Specifically, we first construct a scoring matrix **F** of size $(M+1) \times (L+1)$, where the (m, ℓ)-th entry $F_{m,\ell}$ is the negative minimum edit distance between the first m characters of $\mathcal{P}$ and any sub-sequence $\mathcal{S}_{\ell',\ell} = s_{\ell'} \dots s_\ell$ of $\mathcal{S}$ that ends at position ℓ. The scoring matrix can be constructed recursively:

$$F_{m,\ell} = \begin{cases} 0 & \text{if } m = 0 \\ -m, & \text{if } \ell = 0 \\ \max\left(F_{m-1,\ell-1} - c, F_{m-1,\ell} - 1, F_{m,\ell-1} - 1\right) & \text{otherwise,} \end{cases} \tag{2}$$

where c is the substitution cost that takes a value of 0 if $p_m = s_\ell$ and 1 otherwise. Once **F** is computed, the maximum value in the last row is the optimal score, and the best-matched sub-sequence can be identified through backtracking. The computational complexity is on the order of $\mathcal{O}(ML)$. Since pattern $\mathcal{P}$ is usually much shorter than sequence $\mathcal{S}$, the scoring matrix can be computed efficiently. Moreover, unlike CNN, approximate string matching uses the edit distance to measure the similarity between a pattern and a sub-sequence, *allowing for deletions and insertions*. Thus, it is well suited for extracting pertinent information from biological sequences.

2.3 Novel Neural Network for Approximate String Matching

A major issue with approximate string matching for our application is that patterns of interest are generally unknown and can only be pre-determined heuristically. To address the issue, we propose a novel neural network for approximate string matching that enables the learning of patterns from data *automatically*. To cast the problem into a continuous optimization problem so that the constructed neural network can be trained through gradient descent, some modifications are merited. First, we use one-hot coding to transform an input sequence $\mathcal{S}$ into an $L \times d$ matrix $\mathbf{S} = [\mathbf{s}_1^T, \cdots, \mathbf{s}_L^T]^T$. Here, each letter is represented by a d-dimensional row vector and d is the size of an alphabet ($d = 4$ for DNA sequences and $d = 20$ for protein sequences). Similarly, pattern $\mathcal{P}$ is transformed into an $M \times d$ matrix $\mathbf{P} = [\mathbf{p}_1^T, \cdots, \mathbf{p}_M^T]^T$, where the value of each element can be learned through training (detailed below). Second, we replace the substitution cost c with $-\mathbf{p}_m \mathbf{s}_\ell^T$ to measure the cost of the mismatch between the m-th vector of the pattern and the ℓ-th vector of the input sequence. Third, while in the original algorithm the gap penalty is set to 1, in order to make the constructed neural network more generally applicable, following the work of [26], we set it to be a learnable parameter. Finally, in order for the constructed mapping function to be differentiable, we replace the max function in Eq. (2) with a generalized maximization operator [27], given by

$$\max^{\gamma}(a_1, \cdots, a_J) = \gamma \log \sum_{j=1}^{J} \exp\left(a_j/\gamma\right), \tag{3}$$

where $\gamma > 0$ is a smoothing parameter. With the above modifications, Eq. (2) can be re-formulated as:

$$F_{m,l} = \begin{cases} 0, & \text{if } m = 0 \\ -mg, & \text{if } \ell = 0 \\ \max^{\gamma}\left(F_{m-1,\ell-1} + \mathbf{p}_m \mathbf{s}_\ell^T, F_{m-1,\ell} - g, F_{m,\ell-1} - g\right), & \text{otherwise}, \end{cases} \tag{4}$$

where g is the gap penalty. Using the above-modified approximate string matching, we construct a neural network to map input sequences into embedding vectors. Specifically, given an input sequence $\mathcal{S}$ and N patterns $\mathcal{P}_1, \ldots, \mathcal{P}_N$, we generate N scoring matrices $\mathbf{F}_1, \ldots, \mathbf{F}_N$. We extract the maximum value v_n from the last row of each scoring matrix $\mathbf{F}_n$, and concatenate them into vector **v** to compute an embedding vector

$$\mathbf{u} = \text{ReLU}(\mathbf{v} + \mathbf{b}), \tag{5}$$

where ReLU is the rectifier activation function [28] and **b** is a bias term.

2.4 Learning Parameters through Backpropagation

Finally, we discuss how to estimate the parameters of the proposed method, specifically the patterns used in approximate string matching and the gap penalty, efficiently through backpropagation by minimizing the mean squared error calculated by comparing embedding distances and alignment distances (see Eq. (1)). While backpropagation can be easily implemented by using PyTorch [29], the computation of the gradient of the mean squared error with respect to the patterns is not trivial. Since the patterns are independent of each other, we only need to consider one pattern. Specifically, given pattern matrix **P**, we need to calculate the partial derivative of the mean squared error with respect to each row vector of the pattern matrix

$$\frac{\partial C(\mathbf{\Theta})}{\partial \mathbf{p}_m} = \frac{\partial C(\mathbf{\Theta})}{\partial v}\frac{\partial v}{\partial \mathbf{p}_m}, \forall m \in \{1, \cdots, M\} \ , \tag{6}$$

where v is the maximum value of the last row of scoring matrix **F**. We note that while the computation of **F** depends on an input sequence, only the best-matched sub-sequence of the input sequence is involved in the computation of v. We utilize this fact to develop an efficient scheme for the computation of gradients. By definition, v is the score of the global alignment between the pattern and its best-matched sub-sequence, and thus can be computed by using the Needleman-Wunsch (NW) algorithm [7]. An issue with the NW method is that its output is not differentiable. To address the issue, we resort to the differentiable Needleman-Wunsch algorithm [26] to approximate the value of v and compute the partial derivatives with respect to the pattern and the gap penalty. Let $\tilde{\mathcal{S}}$ be the best-matched sub-sequence, and $\tilde{\mathbf{S}} = [\tilde{\mathbf{s}}_1^T, \cdots, \tilde{\mathbf{s}}_{\tilde{L}}^T]^T$. We construct an $(M+1) \times (\tilde{L}+1)$ scoring matrix $\tilde{\mathbf{F}}$ for the differentiable Needleman-Wunsch algorithm:

$$\tilde{F}_{m,\ell} = \begin{cases} -\ell g, & \text{if } m = 0 \\ -mg, & \text{if } \ell = 0 \\ \max^{\gamma}\left(\tilde{F}_{m-1,\ell-1} + \mathbf{p}_m \tilde{\mathbf{s}}_\ell^T, \tilde{F}_{m-1,\ell} - g, \tilde{F}_{m,\ell-1} - g\right), & \text{otherwise.} \end{cases} \tag{7}$$

By construction, $\tilde{F}_{M,\tilde{L}} \approx v$. Thus, the approximation of the partial derivative of v with respect to each row of pattern **P** can be computed as:

$$\frac{\partial v}{\partial \mathbf{p}_m} \approx \frac{\partial \tilde{F}_{M,\tilde{L}}}{\partial \mathbf{p}_m} = \sum_{\ell=1}^{\tilde{L}} \frac{\partial \tilde{F}_{M,\tilde{L}}}{\partial \tilde{F}_{m,\ell}} \frac{\partial \tilde{F}_{m,\ell}}{\partial \mathbf{p}_m}, \forall m \in \{1, \cdots, M\} \ . \tag{8}$$

It can be shown that $\partial \tilde{F}_{m,\ell} / \partial \mathbf{p}_m = \exp((\tilde{F}_{m-1,\ell-1} + \mathbf{p}_m \tilde{\mathbf{s}}_\ell^T - \tilde{F}_{m,\ell})/\gamma)\tilde{\mathbf{s}}_\ell$. Note that $\tilde{F}_{m,\ell}$ is involved in the calculation of its three neighbors $\tilde{F}_{m+1,\ell}$, $\tilde{F}_{m,\ell+1}$ and $\tilde{F}_{m+1,\ell+1}$. Hence, $\partial \tilde{F}_{M,\tilde{L}} / \partial \tilde{F}_{m,\ell}$ can be computed recursively. Specifically, when $m \neq M$ and $\ell \neq \tilde{L}$,

$$\frac{\partial \tilde{F}_{M,\tilde{L}}}{\partial \tilde{F}_{m,\ell}} = \frac{\partial \tilde{F}_{M,\tilde{L}}}{\partial \tilde{F}_{m+1,\ell}} \frac{\partial \tilde{F}_{m+1,\ell}}{\partial \tilde{F}_{m,\ell}} + \frac{\partial \tilde{F}_{M,\tilde{L}}}{\partial \tilde{F}_{m,\ell+1}} \frac{\partial \tilde{F}_{m,\ell+1}}{\partial \tilde{F}_{m,\ell}} + \frac{\partial \tilde{F}_{M,\tilde{L}}}{\partial \tilde{F}_{m+1,\ell+1}} \frac{\partial \tilde{F}_{m+1,\ell+1}}{\partial \tilde{F}_{m,\ell}}. \tag{9}$$

Likewise, the partial derivative $\partial v/\partial g$ can be approximated as $\partial \tilde{F}_{M,\tilde{L}}/\partial g$, which can be calculated recursively by taking the partial derivative of Eq. (7) with respect to g. Specifically, when $m \neq 0$ and $\ell \neq 0$,

$$\frac{\partial \tilde{F}_{m,\ell}}{\partial g} = \frac{\partial \tilde{F}_{m,\ell}}{\partial \tilde{F}_{m-1,\ell}} \left(\frac{\partial \tilde{F}_{m-1,\ell}}{\partial g} - 1 \right) + \frac{\partial \tilde{F}_{m,\ell}}{\partial \tilde{F}_{m,\ell-1}} \left(\frac{\partial \tilde{F}_{m,\ell-1}}{\partial g} - 1 \right) + \frac{\partial \tilde{F}_{m,\ell}}{\partial \tilde{F}_{m-1,\ell-1}} \frac{\partial \tilde{F}_{m-1,\ell-1}}{\partial g}. \tag{10}$$

3 Experiments

We performed a large-scale benchmark study to demonstrate the effectiveness and potential utility of the proposed method.

3.1 Sequence Datasets

Table 1 describes the five sequence datasets used in the study. The Qiita dataset was generated from 66 skin, saliva, and fecal samples collected from the Amerindian Yanomami people [30]. It contains 6,734,572 sequences of 151 bps in length, covering the V4 hyper-variable region of the prokaryotic 16S rRNA gene. The RT988 dataset contains 4,119,942 sequences from 90 oral plaque microbiome samples [31]. The sequences have a length of 464-465 bps covering the V3-V4 hyper-variable region of the 16S rRNA gene. Both datasets were generated by Illumina MiSeq, and before analysis, pre-processing comprised of pair-end joining, quality filtering, and length filtering was performed. The Greengenes dataset was extracted from the Greengenes database [32] and contains 925,718 unique full-length 16S rRNA gene sequences with a length ranging from 1,325 to 1,500 bps. The Silva-23S dataset was downloaded from the Silva database [33], containing 39,176 full-length 23S rRNA gene sequences with a length ranging from 2,750 to 3,150 bps. The Zymo dataset was generated from a Zymo mock community sequenced by PacBio circular consensus sequencing technology [34]. We used the *removePrimers* function from the DADA2 R package [35] to remove primers and orient all the sequences in the forward direction. After pre-processing, the Zymo dataset contained 69,367 sequences with a length ranging from 1,187 to 1,518 bps.

3.2 Experimental Setting

We compared our method with seven other alignment-free methods, namely, k-mer [12], ACS [15], Kr [36], FFP [13], kmacs [17], SENSE [19], and NeuroSEED [20]. When evaluating an alignment-free method, estimation accuracy and computational efficiency are the two major considerations. Thus, we calculated the mean relative error (MRE) between alignment distances and distances estimated by an alignment-free method and recorded its computational time. By definition, MRE can be interpreted as the percentage of estimated distances that deviate from alignment distances. Since it is computationally infeasible to align all sequence pairs in a dataset,

Table 1: Summary of the five sequence datasets used in the study.

Dataset	# samples	# reads	sequence length
Qiita	66	6,734,572	151
RT988	90	4,119,942	464-465
Greengenes	N/A	925,718	1,325-1,500
Silva-23S	N/A	39,176	2,750-3,150
Zymo	N/A	69,367	1,187-1,518

we randomly sampled 1,000 sequences without replacement and calculated the alignment distances of all 499,500 possible sequence pairs. The Needleman-Wunsch algorithm [7] with the default setting was used for sequence alignment (match score = 2, mismatch score = -3, gap opening score = -5, gap extension score = -2). To minimize random variations, the above sampling process was repeated ten times. Therefore, we generated ten test datasets from each sequence dataset to evaluate the eight competing methods.

For kmacs, FFP (V3.19), Kr (V2.0.2), and NeuroSEED, we used the source code provided by the associated articles. Since kmacs is an extension of ACS, we used the kmacs binary by setting k = 0 as the implementation of the ACS method. For k-mer, we used our C++ implementation, which is optimized for amplicon sequence data by using a sparse k-mer count representation. For k-mer, kmacs and FFP, different parameters can be applied. Since there is no principal way to estimate the optimal parameter, we tested ten parameters for each method and recorded the best result. For SENSE, we used the default parameters. For NeuroSEED, we used the settings reported to achieve the best results in the original article. For AsMac, we set the number of pattern filters to 300 and the pattern length to 20. For AsMac, SENSE, and NeuroSEED, training of a model for each sequence dataset is required. Since SENSE can only be applied to sequences of roughly equal length, it was trained and tested only on the Qiita and RT988 datasets. To form a training dataset, we randomly sampled sequences from a dataset without replacement and calculated the alignment distances of 5 million sequence pairs. To prevent information leakage, we verified that none of the sequences used for training were included in the test data. The Adam optimizer [37] was employed to train the Siamese neural networks in SENSE and AsMac, where the learning rate was set to 1e-4 and the number of training epochs was set to 200. All experiments were performed on a 3.3 GHz Quad-Core Intel Core i5 with 16GB memory.

3.3 Benchmark Study of Accuracy and Efficiency

First, we applied the eight methods to the Qiita and RT988 datasets, in which sequences cover only a sub-region of the 16S rRNA gene and have similar lengths. Table 2 reports the MREs and CPU time of the eight methods, obtained by averaging over ten runs, and Supplemen-

Table 2: CPU time (seconds) and MRE (%) of eight methods tested on Qiita and RT988 datasets. The numbers in parentheses are standard deviations. When different parameters were used for a given method, the best result is boldfaced. A *p*-value was computed by comparing the MRE result of AsMac with the best result of the other method.

		Qiita			RT988		
Method	Parameter	CPU time	MRE	*p*-value	CPU time	MRE	*p*-value
AsMac	default	16.1 (0.3)	**4.5 (0.1)**	--	21.6 (0.7)	**2.8 (0.1)**	--
SENSE	default	9.7 (0.3)	**5.2 (0.1)**	5.2e-21	18.6 (0.1)	**3.9 (0.2)**	8.0e-12
NeuroSEED	default	6.2 (0.4)	**7.3 (0.1)**	4.5e-23	10.8 (0.5)	**8.7 (0.1)**	3.4e-30
ACS	default	14.7 (0.2)	**51.4 (0.6)**	5.9e-33	44.1 (1.3)	**69.5 (0.7)**	4.7e-34
Kr	default	61.6 (4.3)	**189.1 (8.1)**	3.0e-23	113.8 (1.6)	**22.4 (0.4)**	9.6e-30
kmacs	$k=1$	22.1 (0.6)	21.2 (0.3)		62.7 (1.5)	27.2 (0.2)	
	$k=2$	24.2 (0.5)	**10.2 (0.1)**	5.8e-27	69.8 (1.2)	**16.4 (0.1)**	1.8e-34
	$k=3$	25.8 (0.2)	14.4 (0.2)		76.5 (1.6)	21.6 (0.4)	
	$k=4$	27.6 (0.2)	23.7 (0.2)		82.5 (1.7)	31.2 (0.5)	
	$k=5$	29.5 (0.4)	31.2 (0.2)		88.2 (2.5)	39.0 (0.6)	
	$k=6$	31.6 (0.4)	37.0 (0.2)		93.4 (2.7)	45.0 (0.5)	
	$k=7$	33.1 (0.9)	41.7 (0.2)		96.5 (1.7)	50.1 (0.5)	
	$k=8$	34.5 (0.8)	45.7 (0.2)		100.0 (1.3)	54.1 (0.5)	
	$k=9$	35.9 (1.0)	49.2 (0.2)		104.4 (2.2)	57.1 (0.4)	
	$k=10$	37.0 (0.8)	52.2 (0.2)		108.1 (2.9)	59.6 (0.4)	
k-mer	$k=3$	3.1 (0.1)	**14.9 (0.3)**	3.1e-26	3.3 (0.1)	**36.8 (0.6)**	2.6e-27
	$k=4$	5.3 (0.2)	65.8 (0.6)		8.3 (0.3)	62.7 (1.6)	
	$k=5$	6.4 (0.3)	129.5 (1.1)		14.0 (0.1)	147.8 (1.5)	
	$k=6$	6.7 (0.3)	167.3 (1.4)		16.9 (0.1)	219.1 (1.8)	
	$k=7$	6.6 (0.2)	188.4 (1.7)		17.9 (0.2)	267.6 (2.2)	
	$k=8$	6.5 (0.2)	200.7 (1.9)		18.0 (0.1)	301.4 (2.7)	
	$k=9$	6.5 (0.2)	201.2 (2.0)		18.0 (0.1)	302.1 (2.7)	
	$k=10$	6.5 (0.2)	201.4 (2.0)		17.9 (0.1)	301.0 (2.6)	
	$k=11$	6.5 (0.2)	201.4 (2.0)		17.9 (0.1)	300.0 (2.6)	
	$k=12$	6.4 (0.2)	201.4 (2.0)		17.9 (0.1)	299.0 (2.5)	
FFP	$l=6$	2.9 (0.1)	87.9 (0.2)		2.9 (0.01)	93.0 (0.1)	
	$l=7$	5.0 (0.1)	90.0 (0.1)		4.9 (0.05)	85.4 (0.1)	
	$l=8$	9.8 (0.2)	38.7 (0.3)		9.9 (0.02)	83.2 (0.1)	
	$l=9$	17.4 (0.7)	**38.5 (0.5)**	4.3e-32	18.0 (0.05)	78.0 (0.2)	
	$l=10$	33.2 (1.1)	97.4 (1.0)		35.5 (0.04)	**18.4 (0.5)**	3.1e-25
	$l=11$	61.2 (2.4)	137.5 (1.4)		64.9 (0.05)	95.6 (1.1)	
	$l=12$	121.6 (4.5)	162.8 (1.8)		123.7 (0.4)	169.8 (1.7)	
	$l=13$	233.1 (6.4)	178.9 (2.0)		219.8 (1.0)	220.1 (2.2)	
	$l=14$	428.3 (5.9)	189.4 (2.1)		353.4 (3.4)	251.0 (2.6)	
	$l=15$	692.5 (12.0)	196.4 (2.2)		493.4 (7.0)	274.2 (3.0)	

tary Figs. 1 and 2 present the estimated distances against the alignment distances for the two datasets, respectively. In terms of prediction accuracy, AsMac performed slightly better than SENSE and NeuroSEED and significantly outperformed the best results of all other methods by a large margin on both datasets. In terms of running time, while k-mer is the fastest algorithm, its performance is not comparable to our method.

Next, we applied the competing methods to the Greengenes and Silva-23S datasets, where the sequences are of variable lengths. Since there is no biologically meaningful way to trim sequences to an equal length, SENSE cannot be used. Table 3 reports the MREs and CPU time of the seven tested methods. Fig. 2 and Supplementary Fig. 3 present the estimated distances against the alignment distances for the two datasets, respectively. Similar to the results obtained

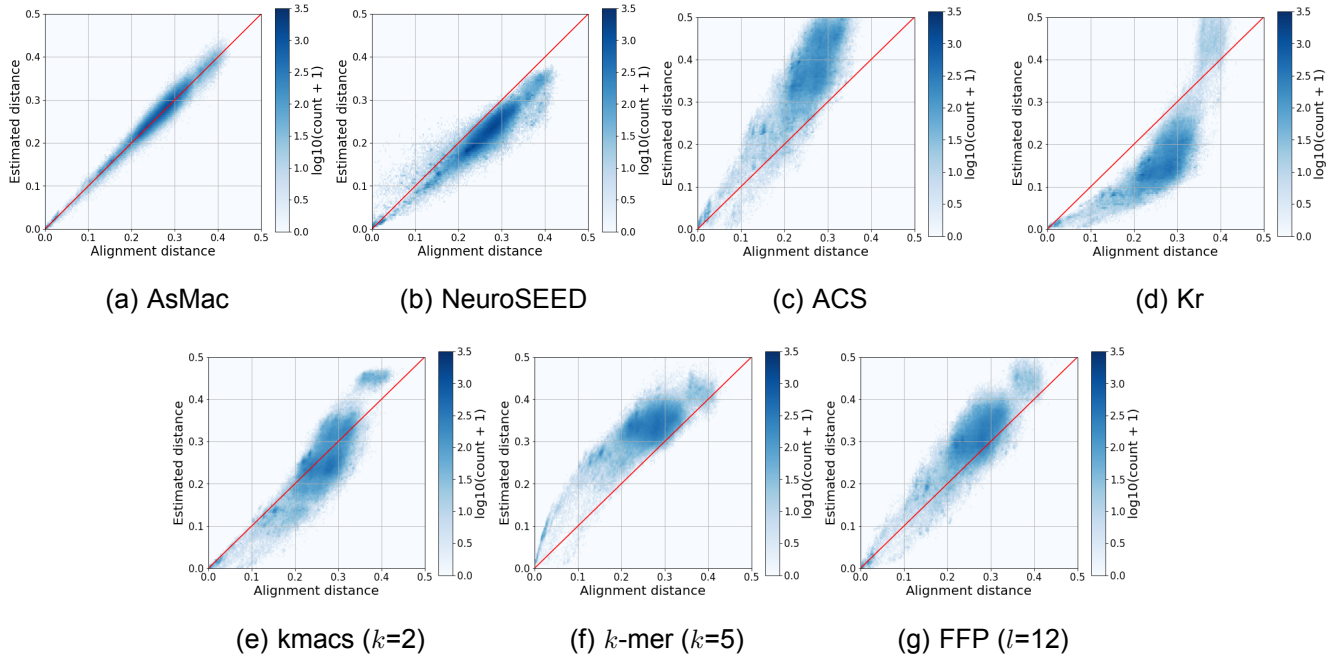

(a) AsMac (b) NeuroSEED (c) ACS (d) Kr

(e) kmacs (k=2) (f) k-mer (k=5) (g) FFP (l=12)

Figure 2: Visualization of alignment distances versus estimated distances computed by seven methods performed on the Greengenes dataset. Each dot represents a sequence pair, and the color of a hex bin represents the number of sequence pairs in the bin. The number in a parenthesis is the parameter that achieved the best result for the corresponding method.

on the Qiita and RT988 datasets, the prediction accuracies of AsMac were significantly better than the best results of all other competing methods.

Finally, we tested the generalization capability of AsMac and NeuroSEED by training a model using the Greengenes dataset and applying it to the Zymo dataset. The results are reported in Table 3 and Fig. 3. Again, AsMac significantly outperformed the other approaches. We noted that, compared to the result obtained from the Greengenes dataset, the prediction accuracy of NeuroSEED declined dramatically. This is likely to be because the Zymo dataset contains a large number of similar sequences that differ by only a few indels, and the CNN structure used by NeuroSEED does not accommodate indels well. As shown in Fig. 3(b), NeuroSEED severely overestimated the pairwise distances of similar sequences. In contrast, by using the ASM structure, our method maintained a high level of accuracy in predicting alignment distances in this situation.

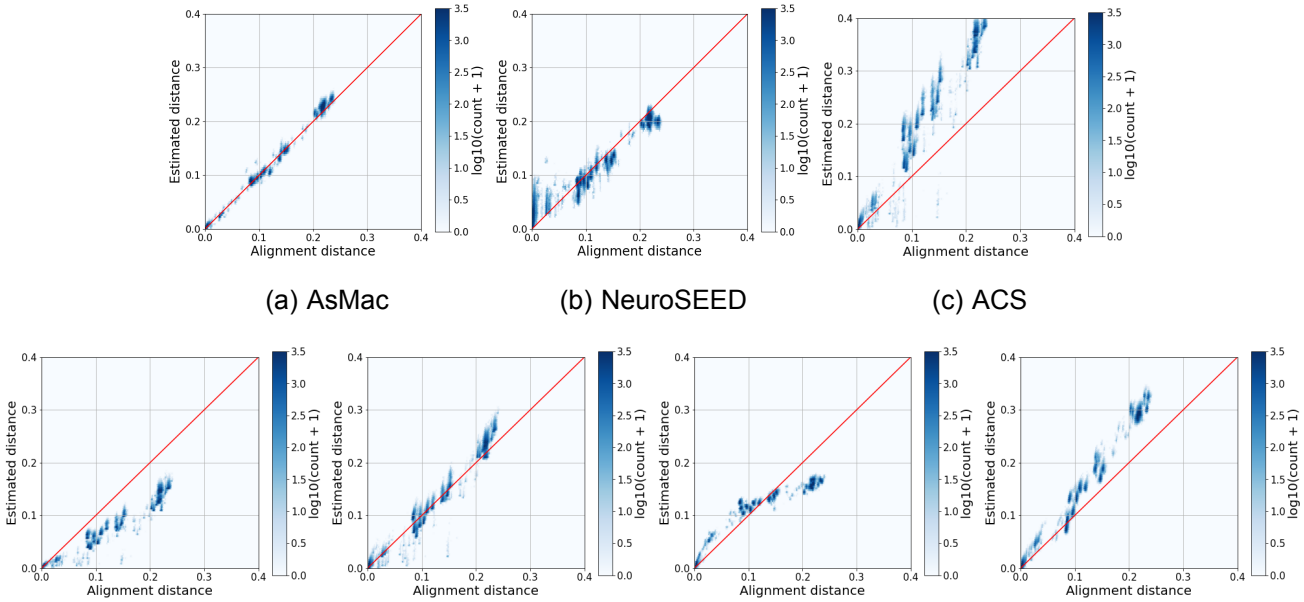

(a) AsMac (b) NeuroSEED (c) ACS

(d) Kr (e) kmacs (k=2) (f) k-mer (k=5) (g) FFP (l=12)

Figure 3: Visualization of alignment distances versus estimated distances computed by seven methods performed on the Zymo dataset. For AsMac and NeuroSEED, a model was trained on the Greengenes dataset and applied to the Zymo dataset.

Table 3: CPU time (seconds) and MRE (%) of seven methods tested on Greengenes, Silva-23S, and Zymo datasets.

		Greengenes			Silva-23S			Zymo		
Method	Parameter	CPU time	MRE	*p*-value	CPU time	MRE	*p*-value	CPU time	MRE	*p*-value
AsMac	default	54.0 (0.9)	**3.6 (0.2)**	--	97.8 (2.3)	**4.0 (0.1)**	--	57.3 (1.0)	**10.6 (0.3)**	--
NeuroSEED	default	22.2 (1.2)	**17.0 (0.2)**	1.8e-29	65.2 (1.1)	**21.2 (0.3)**	1.1e-29	23.1 (0.9)	**134.0 (3.4)**	1.1e-26
ACS	default	129.0 (3.8)	**43.1 (0.5)**	2.8e-32	277.0 (5.0)	**58.5 (0.4)**	3.3e-36	133.1 (4.6)	**86.9 (0.9)**	2.8e-33
Kr	default	140.2 (8.3)	**41.7 (0.4)**	8.7e-33	162.3 (4.3)	**41.9 (2.1)**	2.1e-21	173.5 (12.3)	**42.0 (0.3)**	3.2e-32
kmacs	$k=1$	189.1 (0.9)	16.8 (0.3)		419.5 (13.1)	30.7 (0.3)		191.3 (0.8)	36.4 (0.7)	
	$k=2$	210.1 (1.7)	**12.7 (0.2)**	1.6e-29	464.2 (7.4)	18.2 (0.3)		214.7 (1.0)	**24.4 (0.4)**	6.5e-27
	$k=3$	229.7 (1.0)	18.0 (0.3)		510.7 (11.7)	**13.0 (0.4)**	2.0e-22	231.9 (0.8)	28.3 (0.3)	
	$k=4$	249.1 (2.8)	25.4 (0.3)		553.5 (9.6)	14.0 (0.4)		248.2 (0.3)	37.6 (0.4)	
	$k=5$	269.7 (4.7)	31.8 (0.3)		594.7 (10.8)	19.8 (0.4)		263.6 (0.3)	44.1 (0.4)	
	$k=6$	294.3 (9.6)	36.8 (0.3)		642.5 (6.0)	25.5 (0.4)		280.7 (0.8)	48.3 (0.4)	
	$k=7$	303.2 (1.9)	41.0 (0.3)		676.2 (8.5)	30.3 (0.4)		293.0 (0.5)	51.9 (0.4)	
	$k=8$	317.3 (2.1)	44.3 (0.3)		708.5 (10.8)	34.5 (0.4)		304.4 (0.2))	55.0 (0.4)	
	$k=9$	342.6 (16.0)	47.2 (0.3)		749.7 (20.8)	38.2 (0.4)		316.8 (0.6)	57.6 (0.4)	
	$k=10$	362.6 (25.1)	49.6 (0.2)		773.2 (9.6)	41.3 (0.4)		327.4 (0.3)	59.7 (0.4)	
k-mer	$k=3$	3.4 (0.01)	67.7 (0.3)		5.84 (0.1)	78.9 (0.4)		3.5 (0.0)	53.7 (0.4)	
	$k=4$	9.9 (0.1)	35.7 (0.3)		14.1 (0.2)	66.6 (0.4)		10.0 (0.4)	**40.1 (0.4)**	2.9e-39
	$k=5$	26.7 (0.2)	**30.1 (0.5)**	8.5e-29	32.2 (0.4)	49.3 (0.4)		26.8 (0.3)	107.0 (1.4)	
	$k=6$	44.0 (0.1)	103.5 (0.7)		46.4 (0.8)	**25.7 (0.5)**	2.5e-28	43.3 (0.1)	200.7 (1.7)	
	$k=7$	51.2 (0.7)	154.2 (0.8)		62.8 (0.9)	41.4 (1.1)		51.0 (0.1)	271.7 (1.9)	
	$k=8$	52.6 (0.5)	181.0 (0.8)		85.3 (3.0)	101.9 (1.4)		53.0 (0.2)	318.9 (2.4)	
	$k=9$	52.3 (0.3)	181.1 (0.8)		85.5 (1.9)	101.9 (1.4)		53.0 (0.2)	318.7 (2.4)	
	$k=10$	52.1 (0.1)	181.1 (0.8)		85.5 (3.1)	101.9 (1.4)		53.0 (0.2)	318.7 (2.4)	
	$k=11$	52.0 (0.0)	181.1 (0.8)		84.7 (2.0)	102.0 (1.4)		53.1 (0.3)	318.6 (2.4)	
	$k=12$	52.1 (0.1)	181.2 (0.8)		84.9 (3.7)	102.0 (1.4)		53.1 (0.3)	318.8 (2.4)	
FFP	$l=6$	3.2 (0.02)	98.1 (0.05)		3.6 (0.8)	98.3 (0.7)		3.1 (0.3)	98.0 (0.0)	
	$l=7$	5.2 (0.2)	96.0 (0.05)		5.9 (0.8)	97.0 (0.7)		5.1 (0.4)	95.6 (0.0)	
	$l=8$	11.0 (0.3)	91.6 (0.1)		12.2 (0.8)	94.6 (0.7)		10.4 (0.8)	90.3 (0.0)	
	$l=9$	19.9 (0.7)	84.7 (0.1)		21.7 (0.8)	90.3 (0.7)		19.2 (1.6)	80.9 (0.1)	
	$l=10$	40.7 (1.0)	93.9 (0.1)		44.0 (0.8)	84.4 (0.7)		39.1 (3.0)	86.9 (0.1)	
	$l=11$	76.1 (0.7)	56.4 (0.2)		84.8 (0.8)	92.5 (0.7)		74.1 (6.4)	57.0 (0.3)	
	$l=12$	149.2 (0.8)	**18.0 (0.3)**	2.6e-29	170.8 (0.8)	55.4 (0.7)		143.1 (11.8)	**42.8 (0.2)**	5.1e-31
	$l=13$	274.1 (0.9)	77.3 (0.4)		311.8 (0.8)	**24.3 (0.7)**	5.3e-27	250.0 (12.1)	128.7 (0.7)	
	$l=14$	527.2 (2.1)	120.0 (0.5)		590.0 (0.8)	96.1 (0.7)		382.4 (2.5)	199.1 (0.6)	
	$l=15$	1031.8 (3.5)	147.1 (0.6)		1126.2 (0.8)	147.6 (0.7)		548.5 (15.4)	274.2 (3.0)	

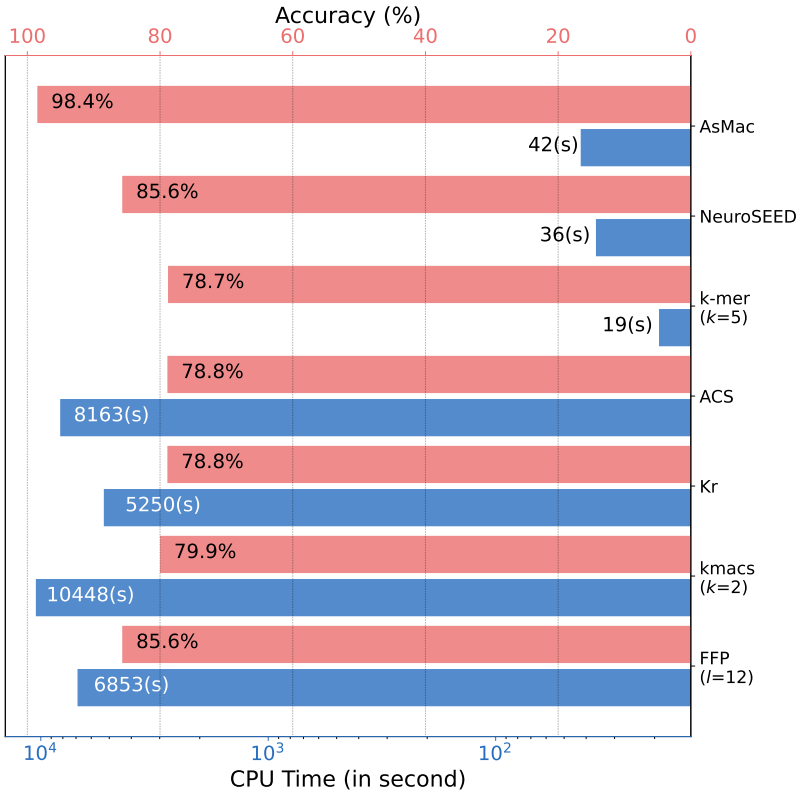

Figure 4: Comparison of taxonomy prediction accuracy and CPU time of seven methods.

3.4 Taxonomy Assignment

To further evaluate the effectiveness and utility of the proposed method, we conducted an experiment where we used our approach to perform taxonomy assignment of a given sequence dataset by searching against a reference database. For the purpose of this study, we constructed a query dataset by randomly sampling 3,000 sequences from the Zymo dataset. We used as the reference database the GG97 dataset, a subset of the Greengenes database [32]. This is the default closed-reference database used by QIIME [38] and contains 30,592 sequences with complete taxonomy annotations at the genus level. We performed a database search using the NW algorithm and annotated each query sequence using the genus of the best-matched reference sequence. We used the result obtained by the NW algorithm as the ground truth and compared the performance of our method with the six competing methods used in the Greengenes study. For kmacs, k-mer and FFP, the parameters were set to be those that achieved the best performance in the Greengenes study. All methods were performed in parallel using 4 threads.

Fig. 4 reports the annotation accuracy and CPU time of the seven methods tested. Our method achieved 98.4% prediction accuracy, outperforming FFP and NeuroSEED by $\sim$13%, and k-mer, ACS, Kr, and kmacs by $\sim$20%. We noticed that kmac did not perform as well as that in the Greengenes and Zymo studies (see Table 3). This may be because for sequence alignment we are concerned about the accuracy of distance estimation for *all* sequence pairs,

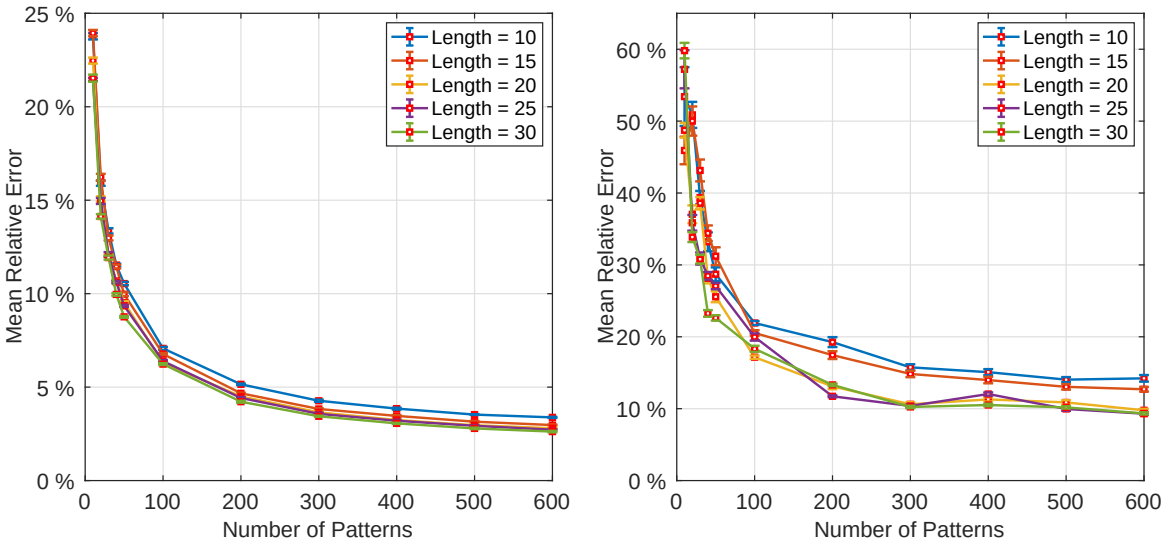

(a) Greengenes (b) Zymo

Figure 5: Parameter sensitivity analysis of the proposed method performed on (a) Greengenes and (b) Zymo datasets.

whereas for sequence annotation we are only interested in sequence pairs that are similar. In terms of computational efficiency, AsMac performed comparably with k-mer and NeuroSEED, but ran two orders of magnitude faster than Kr, ACS, kmacs, and FFP. It is worth noting that, compared to the results reported in Table 2, AsMac, NeuroSEED, and k-mer ran much faster than the other methods. This is because, for the above three methods, the embedding vectors of the reference sequences can be pre-computed, while for Kr, ACS, and kmacs, the pairwise sequence comparison can only be performed in the presence of both query and reference sequences. Although FFP can pre-process the reference sequences, it is computationally expensive to compute the Kullback-Leibler distances between the query and reference sequences.

3.5 Parameter Sensitivity Analysis

The proposed method has two parameters, namely, the pattern number and the pattern length. We performed a parameter sensitivity analysis to investigate how the method performs with respect to the two parameters. We applied the method to the Greengenes and Zymo datasets and reported in Fig. 5 the MRE results obtained by using various pattern numbers and lengths. We can see that, with an increase of the number of patterns, the prediction errors dropped quickly and then flattened when the pattern number was larger than 300. We also observed that our method achieved similar results once the pattern length was larger than 20. For a balance between accuracy and efficiency, we set the pattern number to 300 and the pattern length to 20 as the default parameters.

4 Conclusion

In this paper, we describe a new neural network-based method for alignment-free sequence comparison. The benchmark study demonstrated that the new method is robust against the presence of deletions and insertions and can handle sequences of varying lengths. The taxonomy-assignment experiment showed the value of our method for practical applications. In the current study, we conducted performance testing only on metagenomics sequences. As the future work, we will assess method performance on other homologous sequences. We will also explore the use of ASM for local sequences comparisons, and the aggregation of the ASM structure to form a multi-layer structure, which may further improve prediction accuracy. It will also be of interest to perform in-depth analysis to investigate what type of information in nucleotide sequences has been encoded by the patterns in a neural-network model.

References

[1] Stephen F Altschul, Warren Gish, et al. Basic local alignment search tool. *Journal of Molecular Biology*, 215(3):403--410, 1990.

[2] Robert C Edgar. Search and clustering orders of magnitude faster than BLAST. *Bioinformatics*, 26(19):2460--2461, 2010.

[3] Derrick E Wood and Steven L Salzberg. Kraken: ultrafast metagenomic sequence classification using exact alignments. *Genome Biology*, 15(3):1--12, 2014.

[4] Yijun Sun, Yunpeng Cai, et al. ESPRIT: estimating species richness using large collections of 16S rRNA pyrosequences. *Nucleic Acids Research*, 37(10):e76, 2009.

[5] Yunpeng Cai and Yijun Sun. ESPRIT-Tree: hierarchical clustering analysis of millions of 16S rRNA pyrosequences in quasilinear computational time. *Nucleic Acids Research*, 39(14):e95, 2011.

[6] Wei Zheng, Qi Mao, et al. A parallel computational framework for ultra-large-scale sequence clustering analysis. *Bioinformatics*, 35(3):380--388, 2019.

[7] Saul B Needleman and Christian D Wunsch. A general method applicable to the search for similarities in the amino acid sequence of two proteins. *Journal of Molecular Biology*, 48(3):443--453, 1970.

[8] Andrzej Zielezinski, Susana Vinga, et al. Alignment-free sequence comparison: benefits, applications, and tools. *Genome Biology*, 18(1):186, 2017.

[9] Oliver Bonham-Carter, Joe Steele, et al. Alignment-free genetic sequence comparisons: a review of recent approaches by word analysis. *Briefings in Bioinformatics*, 15(6):890--905, 2014.

[10] Kai Song, Jie Ren, et al. New developments of alignment-free sequence comparison: measures, statistics and next-generation sequencing. *Briefings in Bioinformatics*, 15(3):343--353, 2014.

[11] Andrzej Zielezinski, Hani Z Girgis, et al. Benchmarking of alignment-free sequence comparison methods. *Genome Biology*, 20:144, 2019.

[12] Samuel Kariin and Chris Burge. Dinucleotide relative abundance extremes: a genomic signature. *Trends in Genetics*, 11(7):283--290, 1995.

[13] Gregory E Sims, Se-Ran Jun, et al. Alignment-free genome comparison with feature frequency profiles (FFP) and optimal resolutions. *Proceedings of the National Academy of Sciences*, 106(8):2677--2682, 2009.

[14] Lei Gao and Ji Qi. Whole genome molecular phylogeny of large dsDNA viruses using composition vector method. *BMC Evolutionary Biology*, 7(1):1--7, 2007.

[15] Igor Ulitsky, David Burstein, et al. The average common substring approach to phylogenomic reconstruction. *Journal of Computational Biology*, 13(2):336--350, 2006.

[16] Bernhard Haubold, Peter Pfaffelhuber, et al. Estimating mutation distances from unaligned genomes. *Journal of Computational Biology*, 16(10):1487--1500, 2009.

[17] Chris-Andre Leimeister and Burkhard Morgenstern. Kmacs: the k-mismatch average common substring approach to alignment-free sequence comparison. *Bioinformatics*, 30(14):2000--2008, 2014.

[18] Yang Gao and Liaofu Luo. Genome-based phylogeny of dsDNA viruses by a novel alignment-free method. *Gene*, 492(1):309--314, 2012.

[19] Wei Zheng, Le Yang, et al. SENSE: Siamese neural network for sequence embedding and alignment-free comparison. *Bioinformatics*, 35(11):1820--1828, 2019.

[20] Gabriele Corso, Zhitao Ying, et al. Neural distance embeddings for biological sequences. In *Advances in Neural Information Processing Systems*, pages 1--12, 2021.

[21] Yann LeCun, Yoshua Bengio, et al. Deep learning. *Nature*, 521(7553):436--444, 2015.

[22] Martin Sundermeyer, Ralf Schlüter, et al. LSTM neural networks for language modeling. In *INTERSPEECH*, 2010.

[23] Qiang Wang, Bei Li, et al. Learning deep transformer models for machine translation. *arXiv preprint arXiv:1906.01787*, 2019.

[24] Peter H Sellers. The theory and computation of evolutionary distances: pattern recognition. *Journal of Algorithms*, 1(4):359--373, 1980.

[25] Jane Bromley, Isabelle Guyon, et al. Signature verification using a ``siamese" time delay neural network. In *Advances in Neural Information Processing Systems*, pages 737--744, 1993.

[26] Satoshi Koide, Keisuke Kawano, et al. Neural edit operations for biological sequences. In *Advances in Neural Information Processing Systems*, pages 4960--4970, 2018.

[27] Marco Cuturi and Mathieu Blondel. Soft-DTW: a differentiable loss function for time-series. In *International Conference on Machine Learning*, pages 894--903, 2017.

[28] Vinod Nair and Geoffrey E Hinton. Rectified linear units improve restricted Boltzmann machines. In *International Conference on Machine Learning*, pages 807--814, 2010.

[29] Adam Paszke, Sam Gross, et al. Pytorch: An imperative style, high-performance deep learning library. In *Advances in Neural Information Processing Systems*, pages 8026--8037, 2019.

[30] Jose C Clemente, Erica C Pehrsson, et al. The microbiome of uncontacted Amerindians. *Science Advances*, 1(3):e1500183, 2015.

[31] Robert J Genco, Michael J LaMonte, et al. The subgingival microbiome relationship to periodontal disease in older women. *Journal of Dental Research*, 98(9):975--984, 2019.

[32] Daniel McDonald, Morgan N Price, et al. An improved Greengenes taxonomy with explicit ranks for ecological and evolutionary analyses of bacteria and archaea. *The ISME Journal*, 6(3):610, 2012.

[33] Elmar Pruesse, Christian Quast, et al. Silva: a comprehensive online resource for quality checked and aligned ribosomal RNA sequence data compatible with ARB. *Nucleic Acids Research*, 35(21):7188--7196, 2007.

[34] Benjamin J Callahan, Joan Wong, et al. High-throughput amplicon sequencing of the full-length 16S rRNA gene with single-nucleotide resolution. *Nucleic Acids Research*, 47(18):e103, 2019.

[35] Benjamin J Callahan, Paul J McMurdie, et al. DADA2: high-resolution sample inference from Illumina amplicon data. *Nature Methods*, 13(7):581--583, 2016.

[36] Mirjana Domazet-Lošo and Bernhard Haubold. Efficient estimation of pairwise distances between genomes. *Bioinformatics*, 25(24):3221--3227, 2009.

[37] Diederik P Kingma and Jimmy Ba. Adam: A method for stochastic optimization. In *International Conference on Learning Representations*, pages 1--13, 2014.

[38] J Gregory Caporaso, Justin Kuczynski, et al. QIIME allows analysis of high-throughput community sequencing data. *Nature Methods*, 7(5):335--336, 2010.

Supplementary Data

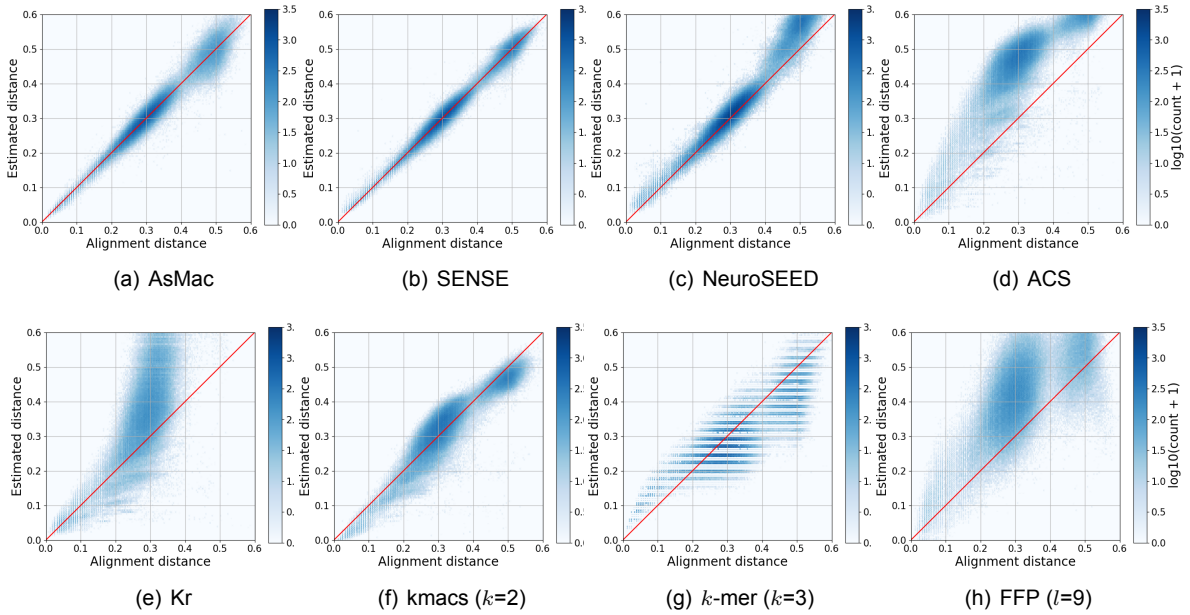

(a) AsMac (b) SENSE (c) NeuroSEED (d) ACS

(e) Kr (f) kmacs (k=2) (g) k-mer (k=3) (h) FFP (l=9)

Figure 1: Visualization of alignment distances versus estimated distances computed by eight methods performed on the Qiita dataset. Each dot represents a sequence pair, and the color of a hex bin represents the number of sequence pairs in the bin. The number in a parenthesis is the parameter that achieved the best result for the corresponding method.

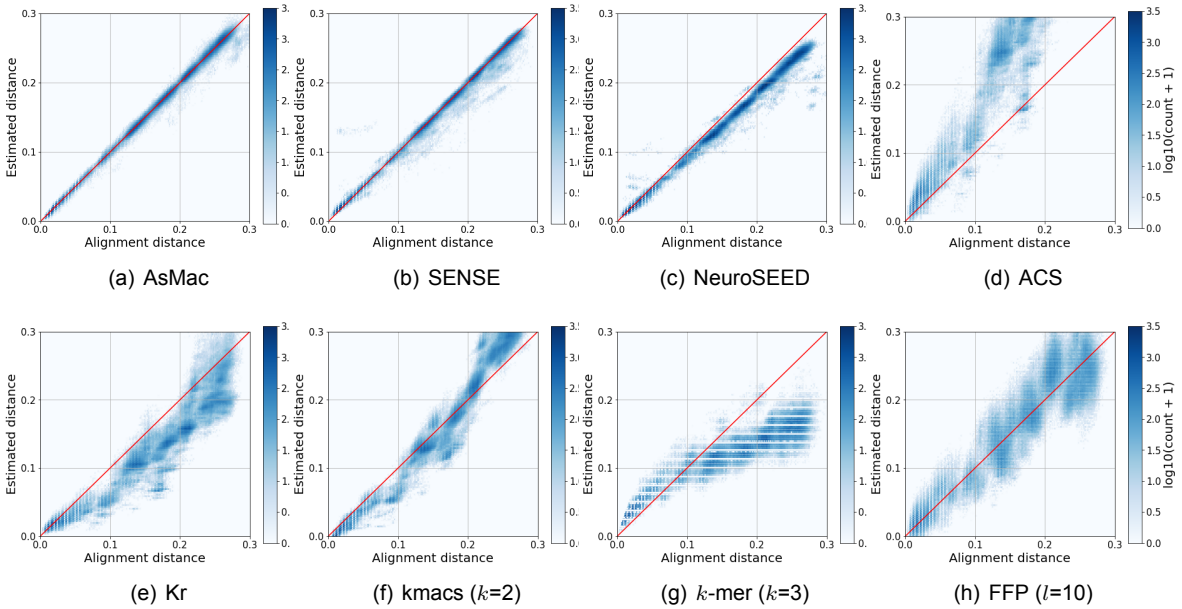

(a) AsMac (b) SENSE (c) NeuroSEED (d) ACS

(e) Kr (f) kmacs (k=2) (g) k-mer (k=3) (h) FFP (l=10)

Figure 2: Visualization of alignment distances versus estimated distances computed by eight methods performed on the RT988 dataset.

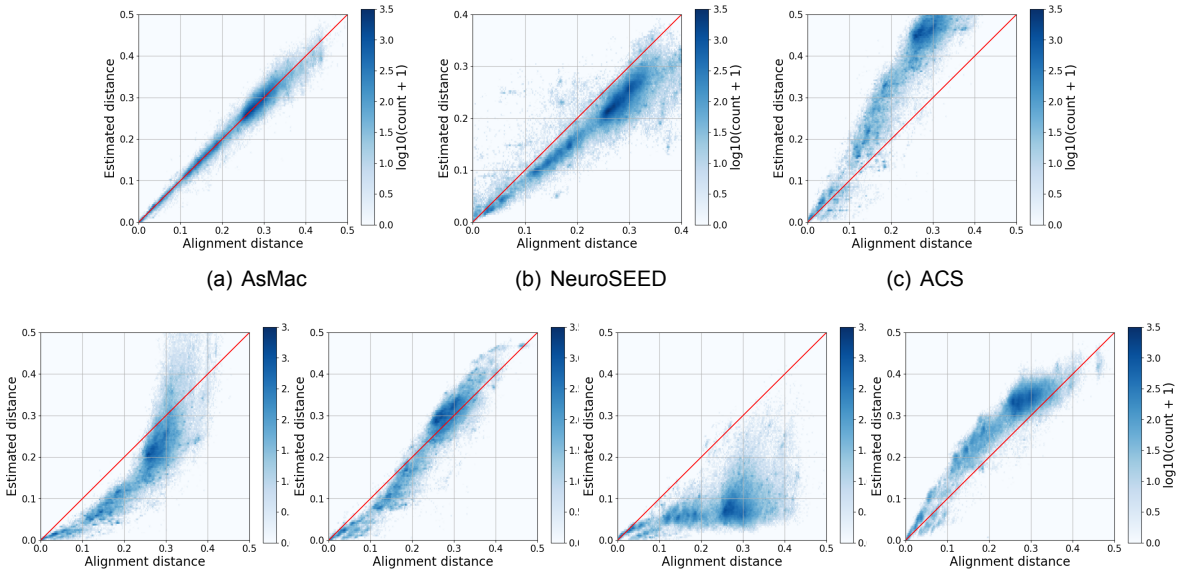

(a) AsMac (b) NeuroSEED (c) ACS

(d) Kr (e) kmacs (k=3) (f) k-mer (k=6) (g) FFP (l=13)

Figure 3: Visualization of alignment distances versus estimated distances computed by seven methods performed on the Silva-23S dataset.